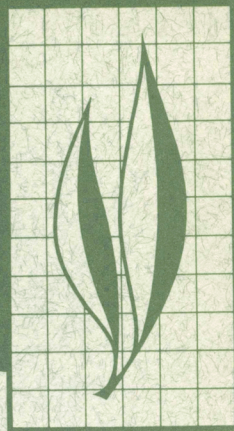


HILGARDIA

A JOURNAL OF AGRICULTURAL SCIENCE PUBLISHED BY
THE CALIFORNIA AGRICULTURAL EXPERIMENT STATION



Volume 47, Number 4 *September, 1979*

Scaling of Field-measured Soil-water Properties

I. Methodology

II. Hydraulic Conductivity and Flux

C.S. Simmons, D.R. Nielsen, and J.W. Biggar



Concepts of similar soil and scaling are applied to investigate the spatial variability of the field-measured soil-water properties, soil-water pressure head, hydraulic conductivity, and soil-water diffusivity associated with unsaturated flow. The classical, analytical aspects of scale factors as regards the invariance of the flow equations expressed in terms of "reduced variables" are reviewed and extended by considering stochastic aspects of random variations in soil-water properties. It is demonstrated that scaling can best be achieved when soil-water properties are represented by a set of related model functions.

The scale distribution is obtained from soil-water pressure head and water content measurements for soil sampling locations 30, 60, 120, 180, 240, and 300 cm below the surface in 12 plots planted to corn. Scale factors are found to have an approximate log-normal distribution.

Methods of computing scale factors directly from soil-water pressure head and hydraulic conductivity measurements and indirectly from soil-water content profiles for a drainage experiment are derived. Improved methods for estimating unsaturated hydraulic conductivity are also presented. Stochastic behavior of flux and cumulative seepage as random functions of the scale factors for a similar soil is described for a simple drainage experiment.

THE AUTHORS:

C.S. Simmons, formerly Post Graduate Research Water Scientist, Department of Land, Air, and Water Resources, Davis, is Research Scientist, Geosciences Department, Battelle Northwest Labs, Richland, Washington.

D.R. Nielsen is Professor of Water Science, Department of Land, Air, and Water Resources, Davis.

J.W. Biggar is Professor of Water Science, Department of Land, Air, and Water Resources, Davis.

TABLE OF CONTENTS

Introduction, 77
PART I. METHODOLOGY
Concepts, 78
Extended scale relations, 79
A general scaling method based on similarity, 81
Statistics of the scaling method, 82
Physical models, 83
Scaling of pressure head and conductivity, 84
Estimation errors in the model parameters, 85
Experimental Design, 86
Field experiment, 87
1-m plots, 88
Results and Discussion: Scaling Soil-water Pressure, 88
One-meter plots: scaling of pressure head, 89
Field experiment: scaling of pressure head, 91
A statistical test of scaling, 92
Estimation errors in the scale factors, 95
Spatial variability with depth, 96
Distribution of scale factors, 98
Summary and Conclusions, 102
PART II. HYDRAULIC CONDUCTIVITY AND FLUX
Calculation of Conductivity: Theoretical, 103
Direct method, 103
Finite difference estimates of $K(v,z)$, 104
Analytical estimates of conductivity, 105
Regression of depth-averaged water content, 107
Unit hydraulic gradient drainage equation, 107
Scaling of Conductivity, 108
Conductivity models, 108
Conductivity scale relation, 109
Scaling in terms of water content, 110
Indirect scaling of flux, 111
New scale relations, 112
Indirect estimate of conductivity, 113
Corrected Estimates of Conductivity, 114
Conductivity based on estimate of pressure head gradient, 114
Conductivity based on scaled drainage flux, 115
Solution of the drainage equation, 116
Millington-Quirk Conductivity and Scaling, 117
Introduction, 117
Modifications to Millington-Quirk conductivity, 118
Matching factor, 118
Computer program for Millington-Quirk conductivity, 119
Scaling, 120

Average Drainage Flux, 120
Local variation of conductivity, 121
Flux as a stochastic function, 121
Average cumulative seepage, 122
Local expected seepage, 122
Spatial variation in seepage, 123
Estimate of average flux, 124
Spatial distribution of flux, 125
Exact statistics of seepage and flux, 126
Spatial Extension of Conductivity, 128
Matching of scale distributions, 129
Results and Discussion: Scaling, 130
Hydraulic conductivity: finite difference estimates, 130
Equality of pressure head and conductivity scale factors, 135
Water-content profiles and cumulative seepage, 136
Indirect scaling of flux, 137
Comparison of scale factors, 140
Hydraulic conductivity: corrected estimates, 141
Millington-Quirk conductivity, 143
Results and Discussion: Flux, 145
Variability of cumulative seepage and flux, 145
Approximate drainage curves, 146
Simulation of experimental field flux, 148
Distributions of water content and flux, 149
Summary and Conclusions, 152

LITERATURE CITED, 154

APPENDICES, 155

ACKNOWLEDGMENTS, 173

Scaling of Field-measured Soil-water Properties^{1,2}

INTRODUCTION

THE PURPOSE OF THE SCALING METHOD is to simplify the description of statistical variations of soil-water properties encountered in the field. Simplification is achieved for particular soil-water properties, such as pressure head, hydraulic conductivity, and diffusivity, by combining the measured data from many soil-sample locations into representative means. By this simplification, the pattern of spatial variability is described by a single scale factor that relates the data measured at each location to those representative means. Another objective of the scaling method is prediction of soil-water flow through an experimental area in terms of the representative means. Thus, scaling is more than a mere averaging process.

With the concept of similar media, Miller and Miller (1956) introduced the analytical aspects of scaling. Similar media differ only in the scale of their internal microscopic geometries, and similar soils would exhibit identical porosities and equivalent particle and pore-size distributions. In the scaling theory, the equations for macroscopic flow in an unsaturated porous medium (Darcy's law and Richards' equation) are expressed as "reduced variables," which are invariant for similar media. Invariance of reduced variables permits comparison of flow systems, which differ by only a scale factor, and scale relations used to define the reduced variables constitute the comparison.

A number of authors² (Miller and Miller, 1955*a* and *b*; Klute and Wilkinson, 1958; Wilkinson and Klute, 1959; Elrick, Scandrett and Miller, 1959; Philip, 1967; Reichardt, Libardi, and Nielsen, 1975) have examined the experimental validity of the scale relations. For soils, the relations seemed to hold only for simple, non-structured sands. Recently, Peck, Luxmoore, and Stolzy (1976) approximated the spatial variability of a watershed area by assuming a normal distribution of scale factors. Warrick, Mullen, and Nielsen (1977*a*) investigated spatial variability in terms of the scale distributions obtained by scaling field-measured soil-water pressure head and hydraulic conductivity. Their work shows that invariant reduced variables represent mean soil water properties when the scale distribution is normalized over a collection of experimental locations. Thus, with their contribution, the scaling method includes the analytical aspect of transforming the flow equations so that it becomes invariant over similar soil locations—and the stochastic aspect of characterizing spatial variability by a distribution of scale factors.

In their research, Warrick, Mullen, and Nielsen (1977*a*) extended the application range of scaling by estimating scale factors relative to the degree of saturation, with the result that the assumption of identical porosities can be eliminated. Indeed, the scaling method now seems to transcend the original similar soil concept on which it was founded. On the other hand, of course, the method's application must be restricted

¹This manuscript was accepted for publication August 4, 1978.

²The Literature Cited section follows Part II of this paper and can be found on page 154.

to soil locations having some reasonable morphological similarity. The extent of what is reasonable, however, has not as yet been established, and the scaling method requires verification for each experimental region.

The purpose of this study was to extend and to develop further the methodology of scaling and to apply these developments to soil-water properties measured in the field during a drainage experiment with a design described earlier by Nielsen, Biggar, and Erh (1973). In particular, the scaling of soil-water characteristic curves and hydraulic conductivity is demonstrated. Techniques are presented for obtaining scale factors indirectly from the measurement of transient soil-water content profiles without recourse to tensiometer measurements, and for computing hydraulic conductivity values without complete hydraulic gradient profiles. Such methods have special interest due to a substantial reduction in collection of data required to evaluate soil-water transport through a field.

Importance of the spatial variability of soils in prediction of water and solute movement is well known (Nielsen, Biggar, and Erh, 1973; Biggar *et al.*, 1977). Because an estimate of water movement below a crop root zone is of prime importance, examples of cumulative seepage and flux within a soil profile as random functions of the scale factors are provided. These examples use approximate drainage equations applied with the same objectives by other authors, (Nielsen, Biggar, and Erh, 1973; Warrick, Mullen, and Nielsen, 1977*b*) but use a different method—namely, the hydraulic conductivity measured in the small drainage experiment is transferred to the larger corn field by the scale distribution.

Before proceeding with the description of experimental design, the original analytical concept of scaling (Miller and Miller, 1956) will be presented and extended from a consideration of soils having similar internal geometry to soils having similar soil-water properties.

I. Methodology

Concepts

The analytical aspect of scaling is that the equations for macroscopic flow in an unsaturated medium (Darcy's law and Richards' equation) are expressed in terms of reduced variables, which are invariant over similar media. Similar media differ at most by a scale magnification of internal geometries. Representation in terms of reduced variables permits comparison of flow systems which differ by only a scale factor. The scale relations provide the means for that comparison.

The scale relation for soil-water pressure head h is

$$h_m(\theta) = \alpha h(\theta) \quad (1)$$

where h_m denotes the reduced head, and α is a scale factor that relates h_m to the pressure head h at each soil location, for each water content θ . This relation is a consequence of variance of the capillary surface tension equation for similar liquid interface geometries (Miller and Miller, 1956). According to (1), the water retention curves of similar soils can be reduced to a single curve by means of scaling the capillary potential at each water content. Each scale factor can be viewed as the ratio of a local microscopic characteristic length and a mean characteristic length. Existence of such a characteristic length scale depends on the validity of the similar media concept: similar soils have similar microscopic geometries.

Invariance of Stoke's equation for similar microscopic flow within a capillary pore system implies that the scale relation for hydraulic conductivity is

$$K_m(\theta) = K(\theta) / \alpha^2 \tag{2}$$

where K_m denotes the reduced conductivity. Scaling theory requires that the reduced conductivity and pressure head scale factors be equal.

Water content θ , being a ratio of volumes, is an inherently reduced variable. At soil locations having equal reduced pressure head, the water contents should be equal for similar soils, inasmuch as the scale relations (1) and (2) include the assumption of identical porosities (saturated water contents).

Scale relations leave the relative magnitude of scale factors and reduced variables arbitrary. Their magnitudes are fixed by choosing a characteristic length and imposing a normalization condition on the scale factors, such as the average of scales over locations equals unity. This normalization condition is implied by the concept of scales being equal to the ratio of characteristic lengths.

Using the scale relations (1) and (2), the equations for one-dimensional vertical flow take the following reduced forms. Darcy's law becomes

$$\frac{L}{\alpha} J = - \frac{K}{\alpha^2} L \frac{\partial}{\partial z} [\alpha z + \alpha h], \tag{3}$$

and the continuity equation becomes

$$L \frac{\partial}{\partial z} \left(\frac{L}{\alpha} J \right) = - \partial \theta / \partial (\alpha t / L^2). \tag{4}$$

Then the reduced flux is

$$J_m = \frac{L}{\alpha} J, \tag{5}$$

and reduced time is

$$t_m = \alpha t / L^2 \tag{6}$$

where $L = z/z_m$ is a macroscopic length scale with z_m as a reference depth. In scale homogeneous regions, i.e., α independent of depth z , the flow equations (3) and (4) can be expressed entirely in terms of reduced variables that remain invariant over similar soil locations. Then, subject to similar initial and boundary conditions the flow equations need only to be solved for one representative location when αL is invariant.

Extended scale relations

The concept of similar soils will now be based directly on similarity of soil-water properties, rather than on uncertain soil morphological properties, such as similar internal geometry. A set of soil-sample locations are similar if the soil-water properties can be scaled.

Because soil porosities are seldom equal for different locations, the soil-water properties are expressed in terms of a saturation variable. Hence, extended scale relations for media with geometries that may not be similar take the forms

$$\alpha h(s) = h_m(s) \tag{7}$$

and

$$K(s) = \alpha^2 K_m(s) \tag{8}$$

where s is the degree of saturation, defined as the water content divided by saturated water content ϕ . Expressing the soil-water properties in terms of saturation, θ/ϕ , constitutes an additional scaling rule. The original scale relations hold only if the saturated water contents for each location are equal. If the saturated water contents for each location are not equal, (7) and (8) may each be satisfied for values of α , which are not necessarily the same.

The soil-water properties are each independently similar for a set of R soil locations, if

$$h_r(s)/h_q(s) = a \quad (9)$$

and

$$K_r(s)/K_q(s) = b \quad (10)$$

hold for all s , for each pair $r, q = 1, \dots, R$ where a and b are constants, depending only on the pair of locations r and q . Thus, the graphs of similar soil-water properties have similar shapes. Note that this definition of similarity could include any other soil-water property, such as soil-water diffusivity. Soil-water properties that satisfy (9) and (10) can be scaled independently, i.e., reduced; however, the scales used to define each reduced variable with the scale relations (7) and (8) need not be equal (i.e., b^2 may or may not be equal to $1/a$).

The principle of scaling is valid for a collection of R soil locations when the soil-water properties are all similar and the scales α_r satisfy the scale relations (7) and (8) with the constraint

$$\frac{1}{R} \sum_{r=1}^R \alpha_r = 1. \quad (11)$$

If the scales satisfy the normalization condition (11), then the reduced variables are given by

$$\frac{1}{h_m} = \frac{1}{R} \sum_{r=1}^R \frac{1}{h_r} \quad (12)$$

and

$$\sqrt{K_m} = \frac{1}{R} \sum_{r=1}^R \sqrt{K_r}. \quad (13)$$

The reduced variables are not the arithmetic means of their respective properties; they will be called scale means. For independently scaled soil-water properties, the scale means are determined by (12) and (13), even if the scales for pressure head and conductivity are not equal. Equations (12) and (13) imply that the normalization condition (11) holds for each property.

The normalization condition (11) has no effect on the similarity of soil-water properties and could be replaced by another condition. Only the definitions of scale means and magnitudes of scales would be altered. But the fundamental character of the scale factor distribution would not be changed. In particular, the distribution of the logarithm of the scale is only shifted by a change in scale means. An example of another normalization condition is that the geometric mean scale equal 1. This is a useful condition if the scale distribution is log-normal.

A general scaling method based on similarity

In the section just preceding, two particular soil-water properties were used to demonstrate the extended scale relations. Here, a general method to scale each soil-water property independently is presented. Let W denote any soil-water property such as pressure head, conductivity, or diffusivity. A physical model function that describes a particular soil-water property is represented by $\hat{W}(s)$. The model function depends on a certain fixed set of parameters with values depending on each soil location. For R soil locations, the scale relations for soil-water properties have a general form:

$$\alpha_r^p \hat{W}_r(s) = W_m(s) \tag{14}$$

where W is a particular scaled soil-water property and p is a constant exponent depending on the associated scaling rule (e.g., $p = 1$ for pressure head, $p = -2$ for conductivity, and $p = -1$ for diffusivity). The physical model function $\hat{W}_r(s)$ for each location r is similar to the scale mean (reduced) function $\hat{W}_m(s)$. Therefore, the model functions must have the form

$$\hat{W}_r(s) = a_r f(s; b_1, \dots, b_k) \tag{15}$$

where the curve shape function $f(s; b_1, \dots, b_k)$ is independent of location. The function $f(s; b_1, \dots, b_k)$ depends on the particular soil-water property being scaled, but the parameters b_1, \dots, b_k are independent of location. Thus equation (15) is implied by the assumption of similarity. Furthermore, the scale mean function must also have the form

$$W_m(s) = a_m f(s; b_1, \dots, b_k) \tag{16}$$

where

$$\alpha_r^p a_r = a_m \tag{17}$$

for all $r = 1, \dots, R$. In similar soil, the parameters a_r depend on the location, and the b_1, \dots, b_k are mutual parameters (common to all locations) that characterize the curve shape.

If a soil-water property W can be scaled according to equation (14), then the scale mean function (16) and scales $\alpha_1, \dots, \alpha_R$ are determined by the constraint (11) as follows:

$$\frac{1}{R} \sum_{r=1}^R \frac{1}{a_r^{1/p}} = \frac{1}{a_m^{1/p}} \tag{18}$$

determines a_m from the a_1, \dots, a_R , and (17) determines the scales $\alpha_1, \dots, \alpha_R$.

A proper choice for the function f depends on the particular soil-water property. The function defined by (15) constitutes a physical model if it describes the measured data, within limits of statistical error, at each location. Furthermore, a physical model should predict the trend of a soil-water property beyond the range of the experimental data sampled. In this respect, a particular model for a soil-water property is termed "physical," that is, not a mere statistical description over the experimental range.

A soil-water property can be scaled with respect to a given choice of physical model (15) if, and only if, a common set of parameters b_1, \dots, b_k can be estimated so that the model function fits the measured data at each location. Partial scaling is fulfilled if the physical model describes the water property data at some locations, but not at all. Finally, two or more soil-water properties can be scaled simultaneously, if each property W can be scaled independently according to (14) and if, furthermore, the scales defined by (17) and (18) for each property W are identical for each location.

Statistics of the scaling method

The scaling method is applied by estimating the model parameters from least squares fit of (15) to measurements at each location. Let s_{ri} and W_{ri} denote $i = 1, \dots, n_r$ measurements of a soil-water property for $r = 1, \dots, R$ locations. Measurement errors ϵ_{ri} for each location are assumed to satisfy the following:

$$\hat{W}_r(s_{ri}) = W_{ri} + \epsilon_{ri} \quad (19)$$

where $E[\epsilon_{ri}] = 0$ and $\text{var}[\epsilon_{ri}] = \sigma_{ri}^2$. Then, assuming homogeneous variances, $\sigma_{ri}^2 = \sigma^2$, the parameters a_1, \dots, a_R and b_1, \dots, b_k can be estimated from the minimum sum of squares,

$$\text{S.S.} = \sum_{r=1}^R \sum_{i=1}^{n_r} [\hat{W}_r(s_{ri}; a_r, b_1, \dots, b_k) - W_{ri}]^2. \quad (20)$$

This condition yields a best least-squares fit of the physical model $\hat{W}_r(s)$ at each location, under the restriction of similarity. An estimate of σ^2 at each location can be obtained from the minimum sum of square of errors at each location. The validity of scaling for the soil-water property can be based on comparison of estimated variance and expected measurement error. Correlations of measured and estimated W can also be used to test scaling. Scaling results can be visualized by plotting the scale-transformed data $\alpha_r^p W_{ri}$ on the graph of the scale mean property given by (16).

In general, the saturation s has experimental error as well as W , and, furthermore, variances of the measurements are seldom homogeneous. This requires minimization of a complete weighted sum of squares (i.e., a chi-square) given by

$$M = \sum_{r=1}^R \sum_{i=1}^{n_r} \left\{ \frac{[\hat{W}_r(\hat{s}_{ri}) - W_{ri}]^2}{\sigma_{ri}^2} + \frac{[\hat{s}_{ri} - s_{ri}]^2}{v_{ri}^2} \right\} \quad (21)$$

where $\hat{s}_{ri} = s_{ri} + \delta_{ri}$, $E[\delta_{ri}] = 0$ and $\text{var}[\delta_{ri}] = v_{ri}^2$.

The minimum function (21) assumes an independent normal distribution for the measurement errors ϵ_{ri} and δ_{ri} ; all covariances equal zero. However, any other minimum function associated with a not necessarily normal likelihood function could be employed in place of (21) if applicable to the particular soil-water property. In any case, the parameters are then determined by the condition of maximum likelihood or minimum for M :

$$\frac{\partial M}{\partial a_r} = 0 \quad (r=1, \dots, R) \quad \text{and} \quad \frac{\partial M}{\partial b_j} = 0 \quad (j=1, \dots, k). \quad (22)$$

Since model functions (15) are usually non-linear in the parameters, special iterative methods are needed to minimize M . A general discussion of such methods is found in Brandt (1976). But a special method applicable to scaling is presented in Appendix A.

Model functions having only one common parameter b were found to be sufficiently accurate for the measured data of this field experiment, and special computer programs for scaling these models were devised (Appendix B).

If the model functions, or transformations of these functions, depend linearly on the parameters, then (22) yields a system of linear equations that can be solved exactly. For example, the parameters of the conductivity model

$$\ln \hat{K}_r = \ln a_r + b_1(s-1) + b_2(s-1)^2 + \dots + b_k(s-1)^k \quad (23)$$

can be determined exactly for

$$M = \sum_{r=1}^R \sum_{i=1}^{n_r} [\ln \hat{K}_r(s_{ri}) - \ln K_{ri}]^2 \quad (24)$$

where K_{ri} ($i = 1, \dots, n_r$) are the measured conductivity for $r = 1, \dots, R$ locations. Here $\ln a_r$ is treated as a new parameter. The minimum function (24) follows from an assumption of log-normal distribution of conductivity with homogeneous variances of $\ln K$ for each location. Such an assumption is equivalent to exponential increase of both mean and variance of conductivity. (Note that the parameters a_1, \dots, a_R , and b of the pressure head and conductivity models are distinct for each physical model, representing statistical parameters, and should not be confused between models.)

Physical models

Scale relations (14) introduced in the previous sections are best verified through application of well defined physical models for the various soil-water properties. Use of arbitrary polynomial approximation tends to cause spurious curve-fitting results. This is especially the case for variable field-measured data.

Two or more physical models for soil-water properties to be scaled simultaneously should be constructed so that they are compatible. As an example, plots of hydraulic conductivity and diffusivity as functions of soil-water content on semi-log graph are often linear, suggesting exponential models for these soil water properties (Nielsen *et al.*, 1973). Thus, the following models are based on empirical observation. Hydraulic conductivity is given by

$$K(\theta) = K_o \exp[\beta(\theta - \theta_o)] \quad (25)$$

and diffusivity is given by

$$D(\theta) = D_o \exp[\delta(\theta - \theta_o)] \quad (26)$$

where θ_o is a particular value of the water content θ . Here, we choose θ_o to correspond to the soil-water content during steady-state infiltration, and, hence, parameters K_o and D_o are the respective steady state values of conductivity and diffusivity. Geometrically, β and δ are the slopes of lines fitting the data plotted on semi-log graphs.

The conductivity and diffusivity are related to the soil-water characteristic curve by the equation

$$D(\theta) = K(\theta) \frac{dh}{d\theta} \quad (27)$$

Integration of (27) using the models (25) and (26) yields the following model function for the soil-water characteristic curve:

$$h(\theta) = A(e^{\rho\theta} - e^{\rho\phi}) \quad (28)$$

where

$$\rho = (\delta - \beta) \text{ and } A = D_o e^{-\rho \theta_o} / K_o \rho. \quad (29)$$

Derivation of (28) used the condition $h(\phi) = 0$ where ϕ denotes the saturated water content. Another form of equation (28) expressed in terms of degree saturation s is

$$h(s) = a(e^{b(s-1)} - 1) \quad (30)$$

where

$$a = \frac{D_o}{K_o \rho} e^{\rho(\phi - \theta_o)} \text{ and } b = \rho \phi. \quad (31)$$

Equation (30) is the model used to verify scaling of soil-water characteristics.

The models (25), (26), and (28) are incomplete to the extent that certain experimentally observed behavior is not described by them. The hydraulic conductivity often does not obey (25) as θ approaches saturated values, while the soil-water pressure head exhibits a capillary fringe (i.e., $d\theta/dh = 0$ near the saturated water content). Such behavior is not included in these models, being only two independent parameter models. The above physical models, however, were found to be adequate for field-measured data. If required, refinements of these models based on other physical behavior could be made.

Scaling of pressure head and conductivity

Soil-water characteristics stemming from field-measured pressure head and soil-water content were scaled by taking saturation s as the dependent variable and pressure head h as the independent variable. Estimated saturation \hat{s} is given by the model (30):

$$\hat{s}_{ri} = 1 + \frac{1}{b} \ln[1 + h_{ri}/a_r] \quad (32)$$

for $i = 1, \dots, n_r$ and $r = 1, \dots, R$. The saturation variances v_n^2 are assumed homogeneous, and the sum of squares of measurement error in h is neglected in the minimum function (21). Then the parameters a_1, \dots, a_R and b are estimated from minimum sum of squares of errors in s . Lastly, the parameters derived by least squares fit are used to estimate the variances v^2 and σ^2 at each location. This simplified approach is similar to standard regression techniques and does not require prior estimates of the variances. Minimization of the sum of squares and calculation of the parameters was performed by a computer program (Appendix B) using an iterative Newton-Raphson method. Initial estimates of the parameters, however, must be provided to the program. Proper order of magnitude for initial parameter estimates and equal a_r proved effective to start the iterations.

The hydraulic conductivity is found to scale effectively with a regression model

$$\ln \hat{K}_{ri} = \ln a_r + b(s_{ri} - 1) \quad (33)$$

and a sum of squares given by (24). Parameters for the model (25) are then obtained for each location by transformation:

$$\beta = b/\phi \text{ and } \ln \hat{K}_o = \ln a + \beta(\theta_o - \phi) \quad (34)$$

A normal distribution of errors in $\ln K$ and homogeneous variances is assumed for each location. The regression (33) estimates the geometric means of conductivity \hat{K} and

steady state conductivity \hat{K}_o . Arithmetic means of conductivity are obtained by transformation to a log-normal distribution as follows. Variance of $\ln K$, denoted v^2 , is estimated from the minimum sum of squares for each location. Then the mean conductivity is

$$K(\theta) = K_o e^{\beta(\theta - \theta_o)} \tag{35}$$

and the deviation is

$$\sigma[K(\theta)] = \sigma_o e^{\beta(\theta - \theta_o)} \tag{36}$$

where

$$K_o = \hat{K}_o \exp(v^2/2)$$

$$\sigma_o = K_o [\exp(v^2) - 1]^{1/2} . \tag{38}$$

By using the model

$$K(\theta) = \bar{K}_o e^{\beta(\theta - \bar{\theta}_o)} \tag{39}$$

where $\bar{\theta}_o$ is an average of θ_o over all locations, the conductivity can be scaled for water content instead of saturation. The same method described above applies, but β is now common to all locations.

Estimation errors in the model parameters

A knowledge of the variances as well as the mean values of scale factors is important for estimating the statistics of transport, such as the flux of water, which depends stochastically on the scales. Estimation of the combined errors in the parameters a_1, \dots, a_R and b of the model (32) that determine the scales is in general a complex calculation involving an $(R + 1)$ dimensional covariance matrix for a non-linear relationship. General methods for solving this problem are discussed by Brandt (1976). However, the following simplified approximate method will provide upper limits for the estimated errors in a_1, \dots, a_R .

Errors in a are computed conditional on the scaling least-squares estimate of b . Thus the common b is assumed known. Let saturation s have a conditional probability-distribution function $P(s|h)$ for each location (see Hald, 1952). That is, P is a function of s , and s , in turn, is functionally related to h . The random variable

$$a(s; h) = h / (e^{b(s-1)} - 1) \tag{40}$$

has expectation given by

$$E[a | h] = \int a(s; h) P(s | h) ds. \tag{41}$$

Deviations of (40) from the estimated mean \bar{a} are given approximately by

$$a(s; h) = \bar{a} + \frac{\partial a}{\partial s} (\bar{s}; h) (s - \bar{s}) \tag{42}$$

where

$$h = \bar{a} (e^{b(\bar{s}-1)} - 1) \tag{43}$$

and \bar{a} equals its least squares estimate, independent of h . Then, standard deviations in

a and s are related by

$$\sigma_a | h = \left| \frac{\partial a}{\partial s} (\bar{s}; h) \right| \sigma_s | h. \quad (44)$$

Using (43), equation (44) becomes

$$\sigma_a | h = \left| \frac{\bar{a}^2 b}{h} (1 + h/\bar{a}) \right| \sigma_s | h. \quad (45)$$

Assuming a uniform distribution of measured pressure head in the interval h_1 to h_2 , the standard deviation of a is

$$\sigma_a = \frac{1}{h_2 - h_1} \int_{h_1}^{h_2} \sigma_a | h \, dh. \quad (46)$$

Assuming homogeneous variance of s, i.e., $\sigma_{s|h}$ equal to the least squares estimate σ_s , (45) and (46) give the following approximate result:

$$\sigma_a = \left(1 + \frac{\bar{a}}{h_2 - h_1} \ln(h_2/h_1) \right) \bar{a} b \sigma_s. \quad (47)$$

Error in the estimated mean \bar{a} is then

$$\sigma_{\bar{a}} = \sigma_a / \sqrt{N} \quad (48)$$

where N is the sample size of measurements for the particular location. Equation (47) indicates that the coefficient of variation of a increases with increased \bar{a} or σ_s and decreases with an increased range of pressure head. Propagation of error in s with h is indicated by equation (45). If $\sigma_{a|h}$ is independent of h, then $\sigma_{s|h}$ increases as pressure head increases.

An estimate of error in the scale factors can be obtained from the error in a. Conditional on a known value of the scale mean a_m , error in the estimated mean scale, $\bar{\alpha}$, is given approximately by

$$\sigma_{\bar{\alpha}} / \bar{\alpha} = \sigma_{\bar{a}} / |\bar{a}| \quad (49)$$

for each location. It can also be shown that the standard deviation of $\ln \alpha$ is given approximately by

$$\sigma_{\ln \alpha} = \left(1 + \frac{\bar{a}}{h_2 - h_1} \ln(h_2/h_1) \right) |b| \sigma_s. \quad (50)$$

Experimental Design

Measurements of soil-water properties used to verify the scaling methodology were obtained from two distinct experiments located at the same site. The first experiment involved measurement of soil-water pressure and soil-water content in a field planted with corn. Objectives of this experiment were measurement of the flux of water and nitrate leaching below the root zone of a crop. This experiment, called the **field experiment**, is located in Davis, California, on a recent alluvial fan classified as Yolo loam and Yolo silt loam. The second experiment, which is called the **1-m plots**, consists of a well-instrumented area within the site of the first experiment and was established with the purpose of estimating hydraulic conductivity in the field. This latter experiment is similar to that described by Nielsen *et al.* (1973) and is called the 1-m plots, because

intense measurements were taken only to a shallow depth of approximately 1 meter. Both experiments were designed to evaluate the effects of spatial variability of a field soil. A brief description of the collected data for each experiment follows.

Field experiment

The experimental field consists of twelve adjacent 18.3 m by 30.5 m plots which are managed as individually irrigated units: three irrigation regimes replicated four times. The water treatments correspond approximately to 1/3, 3/3, and 5/3 of normal evapotranspiration requirements of the corn crop, as determined by several years of experience. These correspond to 20, 60, and 120 cm of irrigation water applied, respectively, during the growing season. Selection of these treatments is based on the objective of providing for three different soil-moisture regimes with corresponding differences in the flux of water that would drain from the root zone. Irrigations are applied at 14-day intervals, providing a quantity of water commensurate with the estimated evapotranspiration requirements. Fertilizer nitrogen is also applied at four concentration levels within each plot, but the effect of this is not considered here.

Soil-water pressure measurements are made using tensiometers placed 30, 60, 120, 180, 240, and 300 cm below the soil surface. Each plot has four tensiometers at each depth, except at 240 and 300 cm where there are a duplicate four at each depth. Water-content measurements are obtained using two neutron probe-access tubes located in each plot. Figure 1 is a diagram of the instrument configuration in each water treatment plot. All instruments are buried at or below the 30-cm depth, so that none protrudes above the soil surface to interfere with cultural practices. This required a modified design, because all tubing is buried within each plot and comes to the surface in the roadways between plots. In addition, a sprinkler system having an unusually narrowly spaced set of sprinkler heads supplies a uniform distribution of irrigation water.

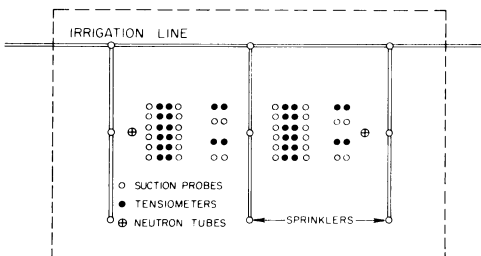


Fig. 1. Diagram of instruments for a single plot of the field experiment, showing relative locations of suction probes, tensiometers, neutron meter access tubes, and sprinkler heads.

Measurements of soil-water pressure are taken immediately before and after an irrigation and in the interval between irrigations. Neutron readings are made at 15 cm intervals to a depth of 300 cm twice a week during the growing season and through the fallow season on a reduced schedule. Simultaneous measurements of soil-water pressure and soil moisture were taken at 98 sample times over an experimental period from 1973 to 1975, covering three crop seasons. Only the data associated with half of the instrument configuration of each plot are used, however. Thus, each water content measurement is associated with two pressure head measurements obtained from the two near lines of tensiometers. These near lines are located 1.1 m and 3.4 m from the one neutron access pipe and are buried in crop rows. Tensiometers are 0.6 m apart along the lines. The resulting two soil-water characteristics are indistinguishable relative to instrument and observer uncertainty and are treated as a single relation for each depth. Hence, there are potentially 196 pairs of pressure head and water content measurements

for each soil sample location specified by plot and depth. But because readings from tensiometers showing defective operation are deleted, the actual number of measurements included in each soil-water characteristic varies. Duplicate measurements for the 240 and 300 cm depths are viewed as representing two additional soil locations for each plot. Thus, there are soil-water characteristic measurements for 96 locations within the 12 plots.

1-m plots

Four 3-meter square plots were established within the field experiment, with the purpose of estimating hydraulic conductivity and flux. These plots are located in the regions between the twelve large plots of the field experiment and are not penetrated by corn crop roots, nor affected by irrigation. Each plot has four neutron probe access pipes installed to the 120 cm depth and three tensiometers installed at 60 cm and 120 cm depths. These probes for measuring soil-moisture and soil-water pressure are symmetrically arranged around the circumference of a one-meter radius circle, with one neutron pipe positioned at the center.

The experimental procedure is to pond water on the plots—a retaining border surrounds each plot for this purpose—until steady state flow is established, as indicated by stable tensiometer readings. When infiltration is complete, the soil surface is covered with plastic, and the plot allowed to drain from this steady-state infiltration condition. Neutron data and tensiometer readings used here are taken daily beginning 1 day after steady infiltration and taken every 2 or 3 days thereafter up to 30 days. Measurements beyond 30 days up to 60 days showed negligible change. Neutron data were taken in 15 cm intervals to 120 cm depth and used to determine water contents from calibrations with soil cores. Thus, each pressure head measurement is the average of three tensiometer readings, and water content is the average of four measurements. Standard deviations for these means represent local variability inherent in the measurement process.

By applying methods similar to those described by Nielsen *et al.* (1973), hydraulic conductivity is estimated for the 60, 75, 90, 105, and 120 cm depths. Water storage in the soil profile is computed for each experimental time and flux estimated directly by finite difference as the time rate of change in storage. An estimate of hydraulic gradient is obtained from the measured pressure head at 60 and 120 cm, and conductivity computed by dividing flux by the hydraulic gradient.

Results and Discussion: Scaling Soil-water Pressure

Before the scaling of pressure head is demonstrated for the field experiment, it is necessary to verify the proposed model function (30) for soil water characteristic curves. The considerable uncertainty of the experimental field measurements owing to limited and scattered data often allows many possible choices for a model characteristic curve. Indeed, an arbitrary or poor choice of model function can result in a predicted mean soil-water characteristic with a physically incorrect shape (e.g., s would not monotonically decrease as h decreases). Scaling results of Warrick, Mullen, and Nielsen (1977a) using polynomials indicate this difficulty with consistent prediction of the mean pressure head. To verify the model function (30), soil-water characteristic data of the 1-m plots are used. This data are not affected by measurement uncertainty typical of the field experiment, such as that caused by irrigation patterns, corn root water extraction patterns, spatial separation of instruments, and hysteresis.

1-m plots: scaling of pressure head

In the case of the 1-m plots, field-measured soil-water characteristics represent only the desorption curve portion of the retention relations at each location. Figures 2 and 3 show the measured soil-water characteristic curves for the 60 and 120 cm depths. Bars indicate the standard deviation of water content. Measured standard deviation of pressure head, which is not shown, is typically between 3 and 6 cm. The pressure head curve in each graph is

$$h(\theta) = a(e^{\rho(\theta-\phi)} - 1) \tag{51}$$

where ρ equals b/ϕ , b is a parameter common to all locations, ϕ denotes saturated water content, and a is a parameter which depends upon each location. The value of a for each location is given by the scale relation

$$a = a_m / \alpha \tag{52}$$

where a_m denotes the scale mean parameter and α is the scale factor. Estimated parameters, saturated water content, normalized scale factors, and standard errors of estimate for the least squares fit of (51) are provided in table 1. In figure 4, the entire pressure head data for the 1-m plots are coalesced according to the scale relation (7), that is, pressure head values are multiplied by the scale factor of the location. The scale mean pressure head curve is described by

$$h(s) = a_m (e^{b(s-1)} - 1) \tag{53}$$

where s , the degree of saturation, equal θ/ϕ . Figure 4 illustrates that all soil-water characteristics are similar and that pressure head can be scaled.

Deviations of measured saturation from the characteristic curves (51 or 53) of each location are not altered by scaling. Therefore, a pooled standard error of estimate of saturation can be obtained for the scaled data. This saturation error corresponds to a water content estimation error equal to 0.007, which is within the limits of measurement error.

We mention without providing details that this scaling method applied to Panoche soil (Nielsen, Biggar, and Erh, 1973), which was previously scaled by Warrick, Mullen, and Nielsen (1977a) yields further verification of the model (51). Also both methods gave approximately the same scale factors.

TABLE 1.

SCALE FACTORS AND STANDARD ERRORS OF ESTIMATE FOR THE SOIL-WATER CHARACTERISTIC CURVES OF THE 1-M PLOTS USING VALUES OF $a_m = -36.2$ AND $b = -5.64$ IN EQUATION (53).

Plot	Depth	α	ϕ	σ_s	σ_h
1	60	0.954	0.45	0.011	12.1
	120	0.585	0.45	0.017	17.5
2	60	1.169	0.44	0.013	9.4
	120	0.922	0.44	0.019	17.8
3	60	0.867	0.44	0.016	12.5
	120	0.984	0.46	0.013	10.3
4	60	1.683	0.45	0.017	14.0
	120	0.837	0.44	0.016	10.6

Standard error of saturation σ_s
 Standard error of pressure head σ_h
 Pooled $\sigma_s = 0.015$

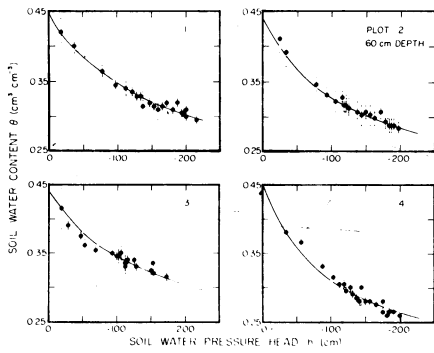


Fig. 2. Soil-water characteristic curves measured at the 60 cm depth in the 1-m plots. Solid lines are given by equation (51).

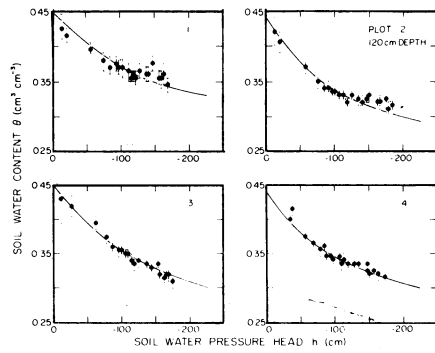


Fig. 3. Soil-water characteristic curves measured at the 120 cm depth in the 1-m plots. Solid lines are given by equation (51).

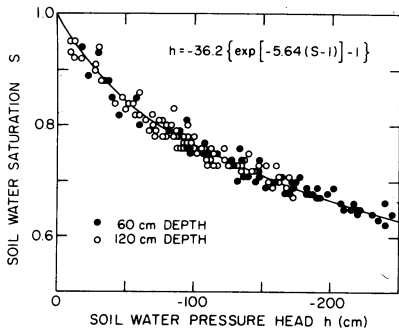


Fig. 4. Scaled soil-water characteristic curve for the data given in figures 2 and 3. Solid circles and open circles represent the 60 and 120 cm depths, respectively, with the solid line given by equation (53).

TABLE 2.

APPROXIMATE SATURATED WATER CONTENTS UNDER FIELD CONDITIONS FOR 96 LOCATIONS IN THE EXPERIMENTAL FIELD. LETTERS A, B, AND C DENOTE IRRIGATION TREATMENTS OF 5/3, 3/3, AND 1/3 ET, RESPECTIVELY.

Plot	Soil Depth (cm)								Treatment
	30	60	120	180	240	300	240	300	
1	0.340	0.362	0.400	0.377	0.416	0.350	0.412	0.369	A
2	0.343	0.360	0.400	0.400	0.418	0.377	0.400	0.363	C
3	0.362	0.377	0.398	0.375	0.378	0.321	0.400	0.371	A
4	0.350	0.353	0.400	0.400	0.300	0.420	0.437	0.418	B
5	0.346	0.366	0.400	0.415	0.381	0.400	0.428	0.380	B
6	0.355	0.362	0.405	0.419	0.428	0.365	0.425	0.400	B
7	0.353	0.362	0.390	0.390	0.363	0.362	0.413	0.418	C
8	0.363	0.371	0.400	0.387	0.362	0.383	0.430	0.400	A
9	0.327	0.362	0.363	0.422	0.433	0.327	0.400	0.400	C
10	0.360	0.378	0.386	0.412	0.427	0.409	0.416	0.383	A
11	0.346	0.366	0.389	0.321	0.319	0.372	0.368	0.413	B
12	0.345	0.359	0.378	0.415	0.350	0.409	0.293	0.428	C

TABLE 3.
ESTIMATED SCALE FACTORS α FOR THE SOIL-WATER CHARACTERISTICS OF
96 LOCATIONS IN THE EXPERIMENTAL FIELD.

Plot	Soil depth (cm)							
	30	60	120	180	240	300	240	300
1	0.350	0.526	0.619	0.603	0.430	5.195	0.620	3.578
2	0.282	0.732	0.516	0.402	0.371	0.932	0.654	0.870
3	0.296	0.492	0.360	1.126	0.375	5.098	1.760	0.790
4	0.263	0.777	0.370	0.324	7.367	0.353	0.663	0.559
5	0.531	0.678	0.462	0.292	1.009	1.165	0.393	0.788
6	0.394	0.580	0.821	0.597	0.421	1.265	0.745	1.957
7	0.344	0.499	0.570	1.746	1.451	0.800	1.287	0.474
8	0.227	0.631	0.497	1.919	5.921	0.572	0.688	0.555
9	0.331	0.481	0.636	0.534	0.497	1.152	0.566	0.528
10	0.446	1.040	0.618	0.378	0.790	0.447	1.004	0.602
11	0.230	1.172	0.707	2.284	1.284	1.302	2.244	0.654
12	0.359	1.391	0.685	0.888	2.428	0.389	1.621	0.384

Field experiment: scaling of pressure head

The pressure head and water content measurements for 96 locations in the plots of the field experiment were scaled with the soil-water characteristic model (51). Because measurements of actual saturated water content were not available for each location, ϕ were estimated from bulk density measurements. Although estimates of the model parameters are affected by use of approximate θ , the scale factors, which represent the relative orientation of characteristic curves, are not appreciably affected. Table 2 contains the approximate saturated water contents, and table 3 contains the scale factors for the field experiment. The parameters of the scale mean characteristic (53) have the following estimates: $a_m = -117$ cm and $b = -4.93$. This scale mean characteristic is based on 13,332 data points, and the pooled standard errors of estimate for saturation and pressure head are 0.038 and 88 cm, respectively.

Scaling of the experimental field data is best visualized by considering the appearance of pressure head and degree saturation data before and after scaling for a single plot. For this purpose, the 8 characteristics of plot 1 were scaled independent of the other 11 field plots. The original data and characteristic curves for each location are shown in figure 5 and the scaled mean characteristic is shown in figure 6. An apparent regularity property of the scaling method is demonstrated for plot 1: the over-all scale factors for the experimental field when restricted to plot 1 and renormalized approximately equal the independently obtained scale factors. That is, the scaling is regular if the results do not change when the method is restricted to a subcollection of soil locations. It should be noted that the values of b (assumed a constant for the field) for the 1-m plots and plot 1 are not numerically identical. This is a consequence of the statistical nature of determining its value from two sets of independent observations. A soil is completely similar over a collection of locations only if the scaling is regular. If scaling is not regular, then the collection of locations might include more than one similar soil class. The scaling of the experimental field's soil-water characteristics appears regular within experi-

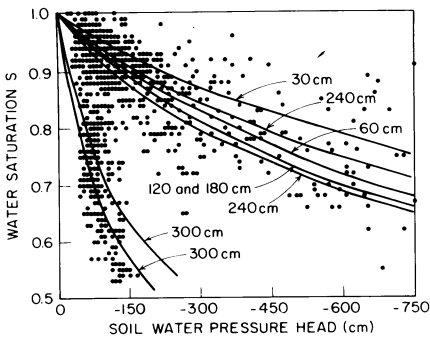


Fig. 5. Soil-water characteristic data for the 30, 60, 120, 180, 240, and 300 cm depths in plot 1 of the field experiment. Solid lines are given by equation (30). Scale factors for the 6 soil depths are respectively 0.249, 0.374, 0.435, 0.432, (0.321 and 0.457), and (3.334 and 2.396). Notice that scale factors were determined for 2 locations for the latter two depths.

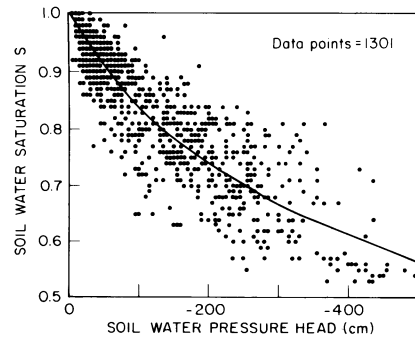


Fig. 6. Scaled soil-water characteristic curve for the data given in figure 5 for plot 1 of the field experiment. Parameters of the curve given by equation (53) are $a_m = -113$ and $b = -3.95$, based on 1301 data points. Standard errors of estimate for degree saturation and pressure head are 0.047 and 57 cm, respectively.

mental error, and it is not necessary to scale separately over individual soil sections, such as those comprised of locations at equal depths.

A statistical test of scaling

Since the experimental field data comprise a large sample with substantial statistical variability, it is not convenient nor rigorous to judge effectiveness of scaling from graphs of moisture and pressure head, as done for the 1-m plots. Instead, scaling is analyzed with the correlation-regression lines of the measured and estimated mean soil-water characteristics. Table 4 contains the statistics for the regression of experimental saturation on estimated saturation for the scaled soil-water characteristic model (53). The ideal situation is a regression line with slope equal 1, intercept equal zero, and correlation coefficient equal 1. Overall, the scaling results for the field experiment approach this ideal. Similarly, the fit of the estimated mean soil-water characteristic for each location is described by a correlation-regression line. Table 5 gives the correlation of experimental and estimated saturation for each location, and the regression line statistics are given in tables 6 and 7. Behavior of residuals for characteristics can be visualized from the regression lines of table 6.

For the intercept approximately equal to zero, positive slopes indicate a majority of measured saturation values above the predicted characteristic curve, and the opposite is indicated by a negative slope. Regression line statistics that depart from the ideal case indicate lack of fit, which is a consequence of factors such as insufficient data to reproduce the characteristic, incorrect data, and invalid similarity model. Two examples are shown in figure 7: (a) is nearly ideal and (b) is a case with poor fit.

The table of correlations provides a convenient method for removing locations that do not satisfy the conditions of similar soil. Evidently, characteristics with low correlation cannot be scaled with the same common parameter b . So scaling is not regular for these locations. Removing locations with correlations less than a prescribed limit improves the scaling results. Most of the locations with low correlation stem from data filling a narrow range of pressure head values and a corresponding wide range of water content values, which results in a nearly vertical soil-water characteristic. Clearly, such characteristics, which occur at the 240 and 300 cm depths, cannot be similar to those described by (51).

TABLE 4.

STATISTICS OF CORRELATION-REGRESSION LINE FOR THE POOLED DATA OF THE EXPERIMENTAL FIELD. REGRESSION OF EXPERIMENTAL SATURATION ON ESTIMATED SATURATION FROM EQUATION (53).

Saturation:	Mean	Standard Error
Experimental	0.8556	—
Estimated	0.8560	—
Slope	0.9970	0.0037
Intercept	0.0022	0.0032
Estimate of S	—	0.0379
Sample Size	13,332	
Correlation Coefficient	0.918	

TABLE 5.

CORRELATION COEFFICIENTS FOR EQUATION (51) FOR 96 LOCATIONS IN THE EXPERIMENTAL FIELD.

Plot	Soil Depth (cm)							
	30	60	120	180	240	300	240	300
1	0.745	0.801	0.899	0.698	0.726	0.695	0.282	0.443
2	0.914	0.968	0.962	0.889	0.827	0.747	0.929	0.707
3	0.897	0.936	0.832	0.770	0.541	0.695	0.724	0.367
4	0.672	0.886	0.913	0.829	0.694	0.122	0.645	0.538
5	0.875	0.907	0.789	0.794	0.543	0.728	0.568	0.622
6	0.892	0.901	0.835	0.745	0.690	-0.073	0.638	0.225
7	0.961	0.840	0.890	0.925	0.820	0.670	0.828	0.621
8	0.834	0.919	0.851	0.699	0.804	0.356	0.504	0.464
9	0.872	0.935	0.904	0.876	0.928	0.744	0.862	0.489
10	0.861	0.884	0.923	0.697	0.625	0.427	0.760	0.253
11	0.776	0.915	0.837	0.813	0.575	0.015	0.758	0.090
12	0.919	0.956	0.844	0.847	0.933	0.329	0.560	0.123

TABLE 6.

SLOPE AND INTERCEPT FOR LINEAR REGRESSIONS OF EXPERIMENTAL SATURATION ON SATURATION ESTIMATED FROM THE SOIL-WATER CHARACTERISTIC EQUATION (51) FOR 96 LOCATIONS IN THE EXPERIMENTAL FIELD. STANDARD ERRORS ARE GIVEN IN BRACKETS.

Plot	Soil Depth (cm)																						
	30	60	120	180	240	300																	
1	0.7912[0.048] 1.371[0.079] 1.104[0.039] 0.797[0.086] 0.943[0.066] 1.234[0.106] 0.260[0.066] 0.843[0.126] 0.1070[0.062] -0.316[0.068] -0.088[0.034] 0.180[0.034] 0.053[0.062] -1.160[0.073] 0.681[0.061] 0.117[0.095]	2	1.274[0.070] 1.548[0.044] 1.060[0.034] 0.755[0.039] 0.071[0.052] 1.136[0.077] 0.760[0.029] 0.896[0.057] -0.245[0.064] -0.439[0.036] -0.050[0.029] 0.216[0.035] 0.117[0.047] -1.114[0.065] 0.203[0.025] 0.245[0.047]	3	1.017[0.045] 1.164[0.033] 0.758[0.037] 0.947[0.065] 0.657[0.076] 0.877[0.082] 1.278[0.089] 0.427[0.081] -0.015[0.041] -0.142[0.029] 0.222[0.034] 0.044[0.054] 0.325[0.073] 0.085[0.058] -0.228[0.074] 0.521[0.074]	4	0.873[0.081] 1.370[0.058] 1.060[0.039] 0.816[0.041] 0.964[0.072] 0.454[0.058] 1.010[0.085] 0.679[0.081] 0.114[0.075] -0.294[0.047] -0.053[0.035] 0.167[0.038] 0.018[0.043] 0.519[0.043] -0.009[0.077] 0.289[0.074]	5	1.277[0.075] 1.661[0.071] 0.891[0.070] 0.779[0.053] 0.737[0.090] 0.933[0.080] 0.692[0.082] 0.986[0.093] -0.227[0.063] -0.529[0.058] 0.094[0.061] 0.198[0.049] 0.222[0.077] 0.057[0.069] 0.207[0.076] 0.013[0.082]	6	0.904[0.038] 1.324[0.048] 0.953[0.049] 0.817[0.062] 1.554[0.123] -0.218[0.222] 0.807[0.072] 0.454[0.149] 0.084[0.035] -0.277[0.042] 0.039[0.042] 0.159[0.054] -0.512[0.114] 1.030[0.188] 0.169[0.063] 0.429[0.110]	7	1.230[0.053] 1.047[0.080] 1.187[0.067] 0.502[0.022] 0.746[0.046] 0.678[0.058] 1.379[0.079] 0.488[0.052] -0.203[0.049] -0.041[0.070] -0.157[0.058] 0.356[0.016] 0.193[0.036] 0.278[0.051] -0.305[0.064] 0.471[0.040]	8	0.875[0.043] 1.142[0.036] 0.709[0.031] 0.858[0.072] 1.101[0.060] 0.505[0.114] 0.755[0.108] 0.524[0.073] 0.115[0.042] -0.121[0.031] 0.259[0.028] 0.107[0.055] -0.065[0.038] 0.459[0.106] 0.218[0.097] 0.435[0.067]	9	1.186[0.084] 1.565[0.068] 1.187[0.067] 0.771[0.044] 1.082[0.042] 0.988[0.070] 1.177[0.059] 0.448[0.072] -0.165[0.076] -0.486[0.059] -0.156[0.056] 0.196[0.038] -0.070[0.037] 0.010[0.058] -0.150[0.051] 0.493[0.065]	10	0.903[0.034] 1.101[0.043] 1.121[0.043] 0.603[0.052] 0.973[0.095] 0.491[0.091] 1.083[0.068] 0.331[0.107] 0.083[0.039] -0.080[0.035] -0.106[0.030] 0.366[0.049] 0.024[0.084] 0.475[0.085] -0.072[0.059] 0.610[0.098]	11	0.870[0.035] 1.533[0.062] 1.106[0.067] 0.669[0.040] 1.121[0.145] 0.025[0.122] 1.194[0.075] 0.100[0.091] 0.117[0.060] -0.406[0.048] -0.087[0.057] 0.227[0.028] -0.090[0.118] 0.020[0.103] -0.145[0.057] 0.820[0.085]	12	1.231[0.077] 1.281[0.046] 0.998[0.067] 1.793[0.111] 0.711[0.031] 0.269[0.109] 0.381[0.053] 0.120[0.093] -0.205[0.070] -0.209[0.035] 0.002[0.057] -0.615[0.087] 0.188[0.021] 0.679[0.102] 0.455[0.040] 0.802[0.085]

TABLE 7.
STANDARD ERROR OR ESTIMATE OF DEGREE SATURATION FOR 96 LOCATIONS
IN THE EXPERIMENTAL FIELD.

Plot	Soil depth (cm)							
	30	60	120	180	240	300	240	300
1	0.049	0.059	0.035	0.038	0.018	0.065	0.027	0.065
2	0.032	0.053	0.020	0.024	0.021	0.032	0.022	0.035
3	0.029	0.023	0.018	0.029	0.018	0.035	0.047	0.021
4	0.049	0.056	0.024	0.022	0.063	0.036	0.031	0.025
5	0.054	0.066	0.036	0.026	0.049	0.029	0.016	0.021
6	0.029	0.031	0.028	0.019	0.026	0.068	0.025	0.048
7	0.029	0.035	0.043	0.046	0.043	0.026	0.048	0.019
8	0.025	0.026	0.023	0.042	0.038	0.022	0.034	0.020
9	0.034	0.039	0.031	0.024	0.024	0.050	0.040	0.033
10	0.037	0.033	0.018	0.016	0.025	0.018	0.025	0.022
11	0.039	0.064	0.050	0.047	0.062	0.040	0.045	0.031
12	0.032	0.035	0.037	0.089	0.036	0.022	0.073	0.021

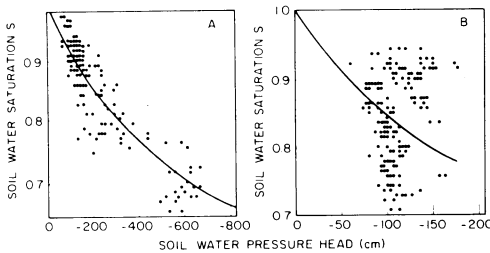


Fig. 7. Examples of soil-water characteristic curves for two selected locations in the field experiment: (a) Plot 1 at 120 cm, 190 data points, standard error of estimate of saturation is 0.034, and correlation coefficient is 0.09; (b) Plot 6 at 300 cm, 184 data points, standard error of estimate of saturation is 0.063, and correlation coefficient is - 0.07.

Estimation errors in the scale factors

The scale factors of table 3 are estimates of the mean scales of local sample distributions. Variation between locations of these scale factors is supposed to represent spatial variability of soil-water properties. But because soil-water characteristic measurements have substantial scatter at each location, the variation in scale values could possibly be a consequence of local variability. Therefore it is necessary to distinguish the component local and spatial variability with estimates of error in the scale factors.

Error in the scale factors is dependent on the estimation error of the model parameters a. Because estimation of combined errors in the parameters a and b is a complex problem for non-linear regression, the following approximate method is used. The entire measurement error in pressure head and water content is transferred to the error in a for each location by computing the error conditional on the regression estimate of b. Then with b equal to its scaling regression estimate, one pair of pressure head and water

content values determines a single value of a from equation (51). In this way the complete measured soil-water characteristic generates a sample distribution of a for each location. By using the scale relation (52), the sample distributions of scale factors are obtained from the distributions of a for each location. Averages and standard deviations of α are then computed for each location from the constructed local distributions. Typically, these local distributions of scales are log-normal.

Table 8 contains average and standard error of average logarithms of α for the constructed scale-sample distributions of each location. The averages and standard errors are computed relative to the same scale mean parameter a_m so that standard deviations of $\ln \alpha$ and $\ln a$ are equal. Scale factors corresponding to average $\ln \alpha$ of the constructed local distributions are not normalized, however. Logarithms of the regression estimated scales given in table 3 are also provided for comparison.

Estimated standard errors given in table 8 can be used to determine which scales are statistically distinct. Here two scales will be viewed as different if the logarithms are separated by at least one standard error. To be more precise, a Student's t-test could be applied to the mean logarithms of scales instead. It is advantageous to compare logarithms of scales rather than scales since the local scale distributions are skewed. Assuming that the local scale distribution is log-normal, standard error of a mean scale factors is given approximately by

$$\sigma[\bar{\alpha}] = \bar{\alpha} \{ \exp(N\sigma^2[\ln \alpha]) - 1 \}^{1/2} / \sqrt{N} \quad (54)$$

where $\bar{\alpha}$ is a mean scale of table 3, N is sample size, and $\sigma[\ln \alpha]$ is the associated standard error of the mean logarithm from table 8. Coefficients of variation obtained from equation (54) have values between 2 and 8 percent.

Spatial variability with depth

Scale factors can be used to describe the spatial variability throughout the soil profile of the experimental field. Figure 8 depicts the average and standard deviation of the logarithm of scales for each depth. Standard deviations for each depth are substantially greater than the standard errors of the means in table 8, which indicates that variation of the scales is mainly due to spatial variability. Coefficients of variation for the spatial component are about a factor of ten greater than those for the local component of the scale variability. Table 9 contains averages and standard deviations of scale factors and coefficients of variation for the local and spatial components of variability.

Figure 8 shows that spatial variability (indicated by length of horizontal bar) increases with depth and manifests an abrupt change at 180 cm, perhaps indicating variation in soil composition over the field. Furthermore, scales generally increase with depth, reflecting a decrease in pressure head for a specified degree of saturation. Thus the experimental field has a scale heterogeneous soil profile; that is, the scale factor is not constant within each plot.

The pooled frequency distribution of the local distributions of $\ln \alpha$ are shown in figure 9 for each depth of the experimental field. These scale sample distributions represent the entire variability at each depth, including both local and spatial components. Scale factors are computed relative to the scaling estimate of a_m . Spatial variability is apparent, judging by the skewness and multi-modal character of the distributions.

TABLE 8.

AVERAGE AND STANDARD ERROR OF AVERAGE $\ln \alpha$ FOR THE SAMPLE DISTRIBUTIONS OF 96 LOCATIONS IN THE EXPERIMENTAL FIELD.

Plot	Soil Depth (cm)							
	30	60	120	180	240	300	240	300
1	-1.0500	-0.6428	-0.4789	-0.5056	-0.8446	1.6476	-0.4787	1.2749
	-0.9879	-0.7003	-0.5220	-0.4477	-0.8346	1.6926	-0.3958	1.3291
	0.0501	0.0414	0.0268	0.0470	0.0270	0.0314	0.0311	0.0326
	130	149	179	87	176	135	183	164
2	-1.2660	-0.3117	-0.6615	-0.9118	-0.9922	-0.0708	-0.4253	-0.1387
	-1.4796	-0.3537	-0.6765	-0.8158	-0.9702	-0.0974	-0.3661	-0.1169
	0.0741	0.0429	0.0241	0.0284	0.0283	0.0220	0.0199	0.0235
	63	66	75	98	134	170	111	145
3	-1.2159	-0.7089	-1.0222	0.1183	-0.9805	1.6288	0.5556	-0.2362
	-1.2257	-0.7268	-0.9636	0.1269	-0.9267	1.6610	0.5342	-0.2019
	0.0384	0.0193	0.0205	0.0220	0.0296	0.0165	0.0282	0.0215
	112	158	190	145	172	119	185	176
4	-1.3364	-0.2518	-0.9930	-1.1281	1.9970	-1.0413	-0.4113	-0.5813
	-1.1516	-0.2152	-1.0434	-1.0962	2.0411	-0.8444	-0.4358	-0.5761
	0.0738	0.0368	0.0278	0.0240	0.0245	0.0839	0.0265	0.0251
	114	121	146	184	182	54	192	173
5	-0.6333	-0.3886	-0.7716	-1.2327	0.0090	0.1525	-0.9347	-0.2388
	-0.7156	-0.3182	-0.6912	-1.1499	0.0095	0.1750	-0.9150	-0.1900
	0.0550	0.0524	0.0282	0.0332	0.0349	0.0252	0.0225	0.0170
	84	79	90	118	163	113	145	153
6	-0.9314	-0.5447	-0.1978	-0.5162	-0.8652	0.2351	-0.2950	0.3712
	-0.8963	-0.5523	-0.2054	-0.5102	-0.8704	0.4350	-0.2782	0.7003
	0.0373	0.0218	0.0221	0.0168	0.0276	0.0380	0.0196	0.0266
	141	154	163	138	156	146	178	165
7	-1.0666	-0.6943	-0.5621	0.5575	0.3723	-0.2230	0.2520	-0.7468
	-1.2981	-0.6466	-0.6067	0.6167	0.4416	-0.1911	0.2448	-0.6687
	0.0742	0.0348	0.0404	0.0295	0.0268	0.0190	0.0308	0.0257
	36	66	80	89	121	165	129	140
8	-1.4830	-0.4607	-0.6985	0.6516	1.7786	-0.5583	-0.3734	-0.5891
	-1.4249	-0.4618	-0.6256	0.6809	1.8152	-0.5272	-0.3881	-0.5529
	0.0385	0.0191	0.0196	0.0228	0.0134	0.0287	0.0352	0.0212
	156	164	192	145	179	134	145	187
9	-1.1069	-0.7320	-0.4528	-0.6281	-0.6996	0.1415	-0.5691	-0.6389
	-1.0654	-0.7331	-0.4472	-0.5921	-0.7166	0.1234	-0.6730	-0.5538
	0.0439	0.0388	0.0310	0.0227	0.0248	0.0328	0.0338	0.0346
	52	65	65	94	104	159	141	123
10	-0.8072	0.0388	-0.4816	-0.9734	-0.2359	-0.8047	0.0043	-0.5074
	-0.7669	0.0472	-0.5143	-0.9232	-0.2387	-0.7790	-0.0198	-0.4872
	0.0368	0.0186	0.0206	0.0239	0.0212	0.0313	0.0218	0.0261
	147	169	118	142	159	133	186	140
11	-1.4694	0.1588	-0.3468	0.8261	0.2497	0.2640	0.8083	-0.4242
	-1.3533	0.1246	-0.3854	0.8550	0.2905	0.3472	0.8437	-0.3755
	0.0548	0.0431	0.0454	0.0248	0.0446	0.0247	0.0215	0.0356
	115	105	105	145	110	160	171	145
12	-1.0246	0.3299	-0.3781	-0.1189	0.8869	-0.9438	0.4831	-0.9578
	-1.1024	0.3152	-0.3617	-0.1865	0.9234	-0.8409	0.5748	-0.9031
	0.0503	0.0268	0.0364	0.0623	0.0242	0.0583	0.0463	0.0285
	45	68	83	91	79	52	111	123

1- LOG OF SCALING REGRESSION ALPHA,
 2- AVG. LOG ALPHA,
 3- STD ERROR OF MEAN LOG ALPHA,
 4- SAMPLE SIZE.

TABLE 9.

COEFFICIENTS OF VARIATION FOR THE SPATIAL AND LOCAL COMPONENTS OF SCALE FACTOR VARIABILITY. LOCAL COEFFICIENT OF VARIATION IS AN AVERAGE VALUE OVER 12 PLOTS EXPRESSED IN PERCENT.

Depth (cm)	Avg. scale	Std. dev.	Spatial C.V.	Local C.V.
30	0.338	0.089	26.3	5.6
60	0.750	0.298	39.7	3.4
120	0.572	0.137	24.0	2.9
180	0.924	0.691	74.8	3.1
240	1.441	1.663	115.4	2.9
300	1.267	1.342	105.9	3.1

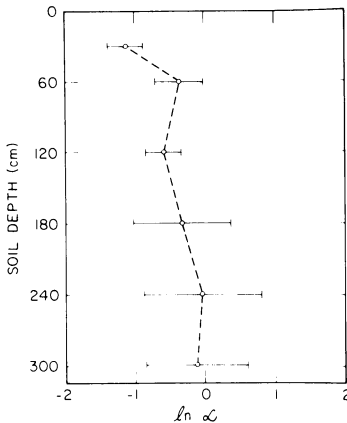


Fig. 8. Average (open circles) and standard deviation (horizontal bars) of $\ln \alpha$ versus soil depth for the 12 plots of the experimental field.

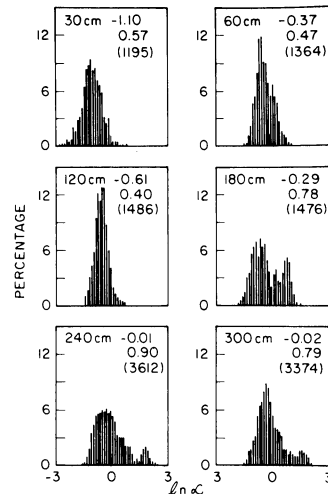


Fig. 9. Pooled frequency distributions for the local sample distributions of $\ln \alpha$ for each depth in the experimental field. Mean, standard deviation, and number, respectively, are indicated for each depth.

Distribution of scale factors

The scale factors for a collection of similar soil locations completely characterize the pattern of spatial variability of soil-water properties. Indeed, a probable outcome for measurements of pressure head and conductivity taken randomly within the soil profile of the experimental field can be determined from the overall scale distribution. Moreover, should the scale distribution of the experimental field prove to be representative of this particular soil-type profile, then estimates of soil-water properties can be deduced for larger regions composed of the same soil-type profile. For these reasons, considerable utility is gained from a simple statistical representation of the scale distribution.

A cumulative probability graph for 72 scale factors estimated for the six depths of the 12 plots of the experimental field is shown in figure 10. The original 96 scale values are reduced to 72 by removing a duplicate scale for each plot at the 240 cm and 300 cm

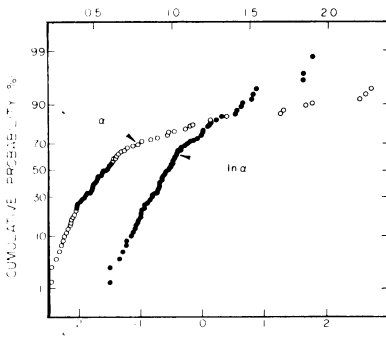


Fig. 10. Cumulative probability graph of 72 values of α and $\ln \alpha$ for the six depths in the 12 plots of the experimental field.

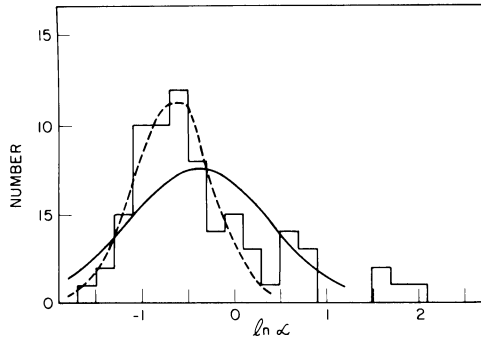


Fig. 11. Frequency distribution for the 72 $\ln \alpha$ values of figure 10. The normal distribution of $\ln \alpha$ indicated by the broken line is based on a mean of -0.6720 and standard deviation of 0.4297 for 61 values of α less than 0.5 . The normal distribution of $\ln \alpha$ indicated by a solid line is based on a mean of -0.3839 and standard deviation of 0.7649 for the 72 values.

depths, and the remaining 72 scales are renormalized. Scales with lowest correlation for each plot are those removed, and those remaining best satisfy the similarity condition. This procedure removes the bias of duplicate depths which would tend to weight the scale distribution for these depths. Locations that show poor scaling results are deleted by the procedure as well.

Figure 10 indicates that the scale factors are not normally distributed but skewed with four values exceeding 4 lying off of the graph. Cumulative probability of $\ln \alpha$ is nearly linear, indicating that the scales are approximately log-normally distributed with a mean of 0.91 , a standard deviation of 0.81 and a mode of 0.38 . A frequency distribution of $\ln \alpha$ for the 72 scales is shown in figure 11 with two estimated normal distributions superimposed: one is determined by the 72 $\ln \alpha$ values and the other by 61 $\ln \alpha$ values with α less than 0.5 . The majority of the 61 scales which compose a cut-off distribution occur for depths less than 240 cm. Evidently the overall distribution is approximately log-normal with a skewed tail representing a few deep locations having extreme scale values. The cut-off distribution of α has a mean of 0.56 , a standard deviation of 0.25 , and a mode of 0.43 , and is considerably less skewed. Table 10 contains the average and standard deviations of α within each plot for the 72 renormalized scales. Plots 1, 3, 4, 8, and 11 seem to be typical samples of the overall distribution with a tail; the other plots are typical samples of the cut-off distribution.

Notice that estimated scale distributions need not satisfy the normalization constraint that the mean α equals 1. However, because scales are only relative quantities, scale distributions can always be renormalized by adjusting the value of the scale mean parameter a_m , without altering predictions of pressure head. This applies also to the sample distributions of figure 9, which are based on single measurement estimates of scales. Indeed, the most important aspect of a scale distribution is the shape. From the distributions of figure 9, it is apparent that extreme scale values originate at the 240 and 300 cm depths.

Scale factors represent the relative orientation of soil-water characteristic curves for similar soil locations and are not merely a consequence of the range of measurements, although the quantity and range of data do influence their estimated values. However,

TABLE 10.
AVERAGE AND STANDARD DEVIATION OF SCALE FACTORS FOR EACH PLOT,
FOR THE SELECTED 72 LOCATIONS IN THE EXPERIMENTAL FIELD.

Plot	Avg. α	Std. Dev. α
1	1.250	1.862
2	0.569	0.229
3	1.478	1.786
4	1.564	2.745
5	0.570	0.302
6	0.772	0.572
7	0.849	0.523
8	1.578	2.123
9	0.588	0.277
10	0.637	0.287
11	1.152	0.845
12	0.994	0.763

for soil locations that have a similar water application history, the scale factors reflect the observed ranges of water content. For example, consider a set of similar soil locations that are dried to the same absolute maximum pressure head, h_{\max} . Then the corresponding minimum saturation, s_{\min} , for each location is determined by α from the scaling model, equations (51) and (52). Saturation s_{\min} decreases monotonically with increases in α . If, furthermore, the lower saturation limits are sufficiently small, the s_{\min} and $\ln \alpha$ satisfy a linear relation given by

$$\ln \alpha = b s_{\min} + A \quad (55)$$

where

$$A = \ln(a_m/h_{\max}) - b \quad (56)$$

Therefore, subject to the above assumptions, the overall distributions of s_{\min} and $\ln \alpha$ are linearly related and inverted with respect to each other. Thus a log-normal distribution of scale factors implies a normal distribution of lower saturation limits, and conversely.

Figure 12 shows a plot of upper and lower saturation limits versus $\ln \alpha$ for two groups of locations. One group is composed of all locations for the depths 30, 60, and 120 cm, and the other is composed of all locations including duplicates for the depths 240 and 300 cm. Within these groups, variation of h_{\max} over locations is relatively small, but the average h_{\max} for each group are different. The letter symbols A, B, and C indicate measurements for the three irrigation treatments of 5/3 ET, 3/3 ET, and 1/3 ET, respectively. Average h_{\max} at each profile depth for the three irrigation treatments are given in table 11. In figure 12, the dash lines represent linear regressions according to (55); the solid lines represent the relationship estimated according to the scaling model, using average $\ln h_{\max}$ for each group of locations. The scaling model predicts a non-linear relationship for s_{\max} greater than 0.7, but because of measurement uncertainty, the approximate linear relationship (55) provides an adequate representation. Deviations of s_{\min} from the ideal relationship are caused by measurement error in saturation and

TABLE 11.
AVERAGE MAXIMUM PRESSURE HEAD FOR EACH OF THE WATER TREATMENTS:
A (5/3 ET), B (3/3 ET), AND C (1/3 ET).

Depth Treatment	30 cm	60 cm	120 cm	180 cm	240 cm	300 cm
A	786 (40)	638 (109)	490 (167)	312 (76)	192 (14)	155 (15)
B	830 (28)	740 (106)	647 (151)	554 (157)	233 (34)	173 (23)
C	780 (26)	758 (36)	725 (10)	682 (18)	561 (109)	266 (90)

(standard deviation)

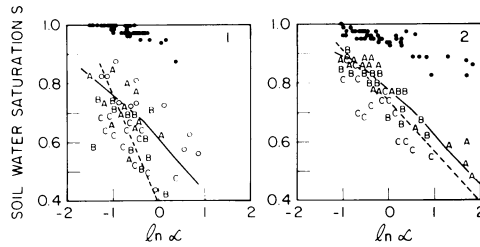


Fig. 12. Saturation limits versus $\ln \alpha$ for two groups of depths in the experimental field. Group 1 is the 30, 60, and 120 cm depths, and group 2 is the 240 and 300 cm depths. Circles indicate values for the 180 cm depth. The letters A, B, and C indicate the three water treatments 5/3, 3/3, and 1/3 of evapotranspiration requirements of the corn crop. Dash line is given by equation (55). Group 1 has $b = -2.58 \pm 0.62$, $A = 1.005 \pm 0.412$, $\sigma_{\ln \alpha} = 0.357$, and $R = -0.58$ for 36 data points. Group 2 has $b = -5.78 \pm 0.42$, $A = 4.249 \pm 0.315$, $\sigma_{\ln \alpha} = 0.357$, and $R = -0.90$ for 48 data points. The solid line curves derive from equations (51) and (52), using an average value of $\ln h_{\max}$ for each group. Solid dots denote all measured upper saturation limits.

variation of h_{\max} between the water treatments. Indeed, for locations having similar scale values, the s_{\min} of the 1/3 ET treatment are consistently less than those of the 5/3 ET treatment, reflecting the increase in h_{\max} with a decrease in applied water, which is indicated by table 11. It is seen in figure 12 that the majority of measured s_{\min} are below the solid line curve. This result is expected because the scaling model estimates the mean of the lower saturation limit, which is usually greater than a single measurement of s_{\min} when the saturation residuals are uniformly distributed about the soil-water characteristic curve. Thus, this result is caused by the degree of uncertainty in measured saturation, relative to the particular model soil-water characteristic curve. Measurements of s_{\min} for the 180 cm depth, which are indicated by "0" in figure 12, form a transition between the other two groups of locations and are usually between the two solid line curves.

Figure 12 indicates also that the scale factors are not correlated with the water treatments, confirming that scales represent soil-water retention properties and not just the range of measurements.

The approximate linear relation (55) provides a useful method for constructing the scale distribution with a reduced quantity of data. First the parameters of equation (55) are estimated by regression for a few locations. Then, the scales of other locations subjected to the same water application can be calculated from only single measurements of minimum saturation. Only enough measurements of entire soil-water charac-

teristics required to establish the range of the regression need be obtained. Of course the method requires locations with similar soil. And this is the assumption that has been verified for the experimental field.

Summary and Conclusions

The model used to describe soil-water pressure represents both absorption and desorption on the hysteresis cycle. Measurement uncertainty makes it impossible to distinguish the cycle curves without including the time dependence. In view of measurement uncertainty, however, a single mean curve seems adequate for describing field-measured soil-water characteristics. No capillary fringe was required in the model.

The soil-water characteristic model used is a two-parameter function which provides a unique relation between soil-water content and soil-water pressure head. But the methodology is not restricted to such a simple model. If further information is available for verification, the method can readily be extended to multi-parameter models, capable of representing complete hysteresis loops. Curve-fitting methods of Brandt (1976) can be applied to make such an extension.

Scaling of the experimental field data gave good results in terms of local correlations, except for a few deep locations where limited ranges in soil-water pressure head yielded nearly vertical characteristic curves, most probably attributed to malfunctioning of tensiometers. In any case, such vertical characteristics yield unit hydraulic gradient, since the capacity equals zero, that is $dh/d\theta = 0$, and they do not affect estimates of the flux.

The scaling method combines data on soil-water properties from many locations and describes the pattern of spatial variability. A final objective of scaling is estimation of water movement over all locations of an experimental field in terms of the scale mean soil water properties.

The soil profile of the experimental field is scale heterogeneous and a single scale does not describe each plot. Therefore the flow equations are not invariant over plots and cannot be expressed entirely in terms of reduced variables—gradients of the scale factors enter the Richards' equation. Thus, flow cannot be computed for each location entirely in terms of scale mean pressure head and conductivity as defined by the Miller-Miller (1956) scaling theory. Moreover, a sink term required by the corn root water extraction would destroy invariance of Richards' equation under a scale transformation.

Some of the objectives of the Miller-Miller theory, however, can be achieved, because in similar soil the variability in pressure head and conductivity can be described by a single scale parameter. Indeed, the flow equations (Darcy's law and continuity equation) can be viewed as stochastic equations that depend on a random variable α . Average storage and seepage (flux) are then obtained by averaging their estimates over the scale distribution. This method is applicable for any sink term included in Richards' equation. Such a stochastic approach has been suggested by Freeze (1975) in another context. A stochastic approach is considered in the next section on scaling conductivity and flux.

For the experimental field, the distribution of scales is approximately log-normal. A sufficient sample size for the number of sites can be estimated for determination of mean soil-water properties and confidence limits. The distribution of scales can describe both the variation of measurements within locations (local sample error) and between locations (spatial variability), and can be used to minimize the number of samples needed to describe the field.